Ion temperature profile importance in collisional sheath modelling

Jung Hern Mun, Magali Muraglia, Olivier Agullo, Cécile Arnas, Lénaïc Couëdel

Ion temperature profile importance in collisional sheath modelling

J-H MUN[1,2], M MURAGLIA[2], O AGULLO[2], C ARNAS[2] and L COUEDEL[1,2]

[1] Department of Physics and Engineering Physics, University of Saskatchewan, Saskatoon, Saskatchewan S7N 5E2, Canada

[2] Aix-Marseille Université, CNRS, Laboratoire PIIM, 13397 Marseille, France

E-mail: jong-hern.mun@univ-amu.fr

September 2022

Abstract.

A plasma fluid model is being developed for the simulation of a direct current plasma discharge simulation including the sheath regions. The code uses a second order centered finite difference scheme and time integration is done by strong stability preserving third order Runge-Kutta method. The separation of scalar and vectorial quantities in two different grids gives stable results. After validation by comparison with theoretical ion sheath profiles, a one dimensional direct current argon discharge was simulated and compared to 1D3v particle-in-cell simulation results. It is shown that the inclusion of a non constant ion temperature profile is mandatory in fluid models in order to recover correct increase of ion velocity in sheaths and thus to simulate direct current (DC) discharges where collisions are not negligible in the sheaths.

1. Introduction

Since its discovery in 1879 by William Crookes, plasma rapidly became one of the base of modern techniques and knowledge through its industrial applications. Besides microelectronics which could not exist without plasma based etching technology, one can also list light source [1, 2], ion thruster [3], protection of aircraft against lightning strikes [4], plasma medicine [5] and even food packaging treatment [6] as notable plasma applications. Its potential is not limited by this non exhaustive list. Plasma is also a potential candidate as a new sustainable energy source involving an international collaboration: nuclear fusion power plants [7, 8].

However, plasma is a very complex system to study because it involves charged particle interactions and related non-linearities. Plasma discharges contains three distinct zones having different physical properties, namely the quasi-neutral bulk plasma, the sheath which is a buffer zone between the plasma and the confining walls in which quasi-neutrality does not hold, and an intermediate transition zone between the bulk and the sheath called pre-sheath [9]. The sheath is the zone of particular interest when studying plasma discharges since this is where the plasma interacts with the boundaries. However, the bulk plasma-sheath transition is still a subject of active research today mainly due to its complex structure [10, 11]. Consequently, the modelling of an entire plasma discharge including the dynamics of sheath is not a trivial problem.

Plasma can be described with different physical models. The microscopic level is the base of Particle-In-Cell (PIC) models. Kinetic models give statistical descriptions via the Boltzmann equation and distribution functions. Finally, the attempt of describing the plasma at a macroscopic level using the first few moments of the Boltzmann equation can be done using a plasma fluid model. With the development of microelectronics, modelling and computer simulation are widely used approaches in plasma physics. PIC and kinetic simulations are usually preferred for their precision since they do not rely on many hypotheses that limit the model applicability, but they demand huge amount of data storage and computational resources [12–16]. On the contrary, fluid models offer better performance at the cost of precision. However, the use of fluid description for a plasma is sometimes questionable. For example, at a very low pressure (usually lower than tenths of pascal), particle interactions (collisions) are not numerous enough to observe equipartition of energy between heavy (neutrals and ions) and light (electrons) particles: they do not have the same temperature. Thus, in many low pressure plasma fluid models, ions are often assumed to be thermalized with the neutral background gas. Also the existence of sheath is another obstacle to overcome since its description demands more physical details than the quasi-neutral bulk plasma (the resolution of the Poisson's equation for the space charge evolution is the very least requirement) and appropriate boundary conditions. Therefore many simulations based on fluid models only describe the quasi-neutral bulk plasma.

Different approaches were employed in order to overcome the limits of a plasma fluid model. Hagelaar et. al. uses a mix of kinetic and fluid approaches called hybrid model [17, 18]. Becker et. al. introduced a four-moments methods for the electrons including the effects of the anisotropic parts of the electron velocity distribution function [19–21]. Sahu et. al. propose to revisit the sheath boundary flux expressions and use an isentropic description of the sheath for improved fidelity [22, 23]. However, it is still common to assume the ions thermalized with the neutrals (consequently a collisionless sheath). In that context a new and reliable numerical plasma fluid model is currently under development in order to be able to simulate accurately and efficiently the sheath region of direct current argon plasma discharges. Under moderate to high pressures ($> 10^1 - 10^2$Pa), we propose to investigate the influence of collisions and ion temperature profile in the sheaths as a perspective to enhance fluid model fidelity. This article presents the preliminary results of a 1D fluid code, focusing on a DC argon (Ar) plasma discharge including the sheath regions. The fluid model and its numerical implementation are presented respectively in Section 2 and Section 3. Then the first results from the fluid code are compared with 1D3v PIC simulation results performed with the commercial code VSIM [24] are presented in Section 4. The current version of the code itself is self-consistent for low temperature plasma discharges with cold ions assumption, but it will be shown that in moderate pressure range (>10Pa), a non constant ion temperature profile (not calculated self-consistently for now) will significantly improve the precision of the result, especially in the sheath region. Finally, in the last section, a conclusion of the present work is given.

2. Fluid model of a DC plasma discharge

2.1. Governing equations

A plasma fluid model is based upon the fact that average macroscopic physical quantities of the system are studied in a similar way to classical neutral fluid. However, a plasma fluid model presents major differences compared to neutral fluid models. A plasma is a fluid constituted of multiple, potentially charged species (at the very least electrons and a positive ion) with radically different physical properties such as their masses and their charges. This obliges the handling of collisional source terms for the ion species (for example, $X + e^- \rightarrow X^+ + 2e^-$). In addition, since the physical medium contains charge carriers, the time evolution of the electromagnetic field needs to be included too. Thus, classical fluid equations such as the Navier-Stokes equations are not applicable. Plasma fluid models are derived from the first few moments of Boltzmann equation coupled to Maxwell equations.

Our model contains two fluids, electrons and Ar^+ ions, in a fixed Ar neutral background. The energy distribution functions of the different species are assumed to be regular under

some hypothesis [25]. The system of plasma fluid equations are as follows:

$$\frac{\partial n_s}{\partial t} + \nabla \vec{\Gamma}_s = S_s, \tag{1}$$

$$m_s n_s \left[\frac{\partial \vec{v}_s}{\partial t} + (\vec{v}_s \nabla)\vec{v}_s\right] = q_s n_s \left(\vec{E} + \vec{v}_s \times \vec{B}\right) - \nabla \overrightarrow{\overrightarrow{P}}_s - m_s n_s f_{ms} \vec{v}_s \left(1 + \frac{S_s}{n_s f_{ms}}\right), \tag{2}$$

$$\frac{\partial (n_e \varepsilon_e)}{\partial t} + \nabla \vec{\Gamma}_{\varepsilon_e} = -\vec{\Gamma}_e \cdot \vec{E} - \theta_e n_e. \tag{3}$$

The first three moments of the Boltzmann equation are used: continuity (Eq. 1), momentum transfer (Eq. 2) and mean energy transfer (Eq. 3) (the last one only for the electrons for now). Here, t is the time, s is an index depending on species (e for electrons and i for ions), n_s is the particle density of the specie s, m_s is its mass, $\vec{v}_s$ its mean velocity, f_{iz} the ionization frequency via electron-neutral collision, f_{ms} the total momentum transfer frequency via particle collisions between s and neutrals, $\vec{E}$ and $\vec{B}$ are the electric and magnetic fields, $\overrightarrow{\overrightarrow{P}}_s$ is the pressure tensor, q_s is the particle charge ($-e$ for electrons and $+e$ for ions, where e is the elementary charge), ε_e is the electron mean energy, θ_e is the energy loss rate via electron-neutral collisions, $\vec{\Gamma}_s = n_s \vec{v}_s$ is the particle flux and $\vec{\Gamma}_{\varepsilon_e} = n_e < \varepsilon_e \vec{v}_e >$ is the electron mean energy flux.
The elastic collisions between electrons-neutrals and ions-neutrals for momentum exchange are taken into account. The only inelastic collisions considered in the model are electron-neutral direct impact ionization collisions. Thus in our model, $S_s = S_e = S_i = f_{iz} n_e$. The ion temperature profile is user-defined. It can be set constant as usually done in low temperature plasma fluid models or a predefined profile can be used.
Poisson's equation completes this model. It is necessary to simulate the space charge distribution evolution inside the plasma:

$$\Delta V = -\frac{e}{\varepsilon_0}(n_i - n_e), \tag{4}$$

which gives the electric field $\vec{E}$:

$$\vec{E} = -\nabla V. \tag{5}$$

A constant electric potential difference is applied between the two electrodes which are the physical boundaries of the system. Thus, the resultant electric field is the combination of external (bias of electrodes) and internal (evolution of space charge) influences.

2.2. Charged species transport

Electron momentum is treated in the drift-diffusion expression as it is commonly done in low temperature plasma models. The electron particle and mean energy fluxes expressed in the drift-diffusion form require transport coefficients which are computed using BOLSIG+ [26–28].

The ion momentum transfer equation cannot be solved in a similar manner. Due to their masses, the ion inertia term cannot be neglected in equation 2. In an attempt to express the ion flux in drift-diffusion form, an *effective* electric field $\vec{E}^{eff}$ can be introduced [29–31]:

$$\vec{\Gamma}_i = n_i \vec{v}_i \equiv \mu_i n_i \vec{E}^{eff} - \nabla(D_i n_i). \tag{6}$$

Furthermore, the time evolution of the mean ion velocity can also be simulated using the effective electric field [32]:

$$\frac{\partial \vec{E}^{eff}}{\partial t} = f_{mi}\left(\vec{E} - \vec{E}^{eff}\right) - f_{iz}\frac{n_e}{n_i}\frac{\vec{v}_i}{\mu_i} - \frac{1}{\mu_i}(\vec{v}_i\nabla)\vec{v}_i. \tag{7}$$

$\left(\vec{E} - \vec{E}^{eff}\right)$ reflects the fact that due to their inertia ions cannot follow the system's electric field $\vec{E}$ evolution in real-time. $\vec{E}^{eff}$ can be interpreted as the real electric field seen with a time delay. This interpretation allows the use of $\vec{E}^{eff}$ in experimental databases to obtain ion mobility $\mu_i N = f(\frac{\vec{E}^{eff}}{N})$ along with Einstein's relation to obtain D_i and f_{mi}. In the literature, these database are available for ions in equilibrium with the applied electric field. The reference database for ion mobility are given in Refs. [33, 34]. They give the values of ion mobility as a function of the equilibrium reduced electric field. This database is well fitted by the empirical Frost's formula [35]. A modified version of Frost's formula taking into account the dependence of ion mobility on ion temperature [36] is used in this work.

2.3. Boundary conditions

The model describes the quasi-neutral plasma and the non-neutral sheath in an self-consistent way, where sheath evolution is stimulated by the boundary conditions. The plasma is bounded by two conducting electrodes where boundary conditions on fluxes and electric potentials are imposed: a grounded anode ($V = 0$) and a negatively biased cathode ($V = -V_c$). The ion flux normal to the boundary is given by the following expression [32]:

$$\vec{\Gamma}_i = \frac{1}{4} n_i \vec{v}_{thi} + \delta \mu_i n_i \vec{E}^{eff}, \tag{8}$$

where $v_{thi} = \sqrt{\frac{8 k_B T_i}{\pi m_i}}$ is ion thermal velocity and δ is n integer equal to 0 or 1 depending on the orientation of the effective electric field:

$\delta = 1$ if $\vec{E}^{eff}$ brings ions to the wall

$\delta = 0$ otherwise.

There are two components in the boundary ion flux: thermal diffusion flux which always exists and drift flux induced by $\vec{E}^{eff}$ only when it is oriented towards the wall.
The electron flux normal to the boundary has a similar expression:

$$\vec{\Gamma}_e = \frac{1}{4} n_e \vec{v}_{the} + \delta \mu_e n_e \vec{E}, \tag{9}$$

where $v_{the} = \sqrt{\frac{8 k_B T_e}{\pi m_e}}$. However, the electron flux has an additional term at the cathode boundary which reflects the secondary emission due to ion impact:

$$\vec{\Gamma}_e^{2nd} = -\gamma_i \vec{\Gamma}_i. \tag{10}$$

The secondary emission coefficient γ_i is set to 0.1 according to Ref. [37]. For the electron mean energy flux, the expressions are similar with the particle density n_e replaced by the energy density $n_{\varepsilon_e} = n_e \varepsilon_e$:

$$\vec{\Gamma}_{\varepsilon_e} = \frac{1}{4} n_{\varepsilon_e} \vec{v}_{the} + \delta \mu_{\varepsilon_e} n_{\varepsilon_e} \vec{E}. \tag{11}$$

Similarly, it has an additional term in the cathode:

$$\vec{\Gamma}_{\varepsilon_e}^{2nd} = \vec{\Gamma}_e^{2nd} \varepsilon_e^{2nd}, \tag{12}$$

where the secondary electrons are considered to have a constant mean emission energy of $\varepsilon_e^{2nd} = 3\text{eV}$ which lies between the range of $2 - 6\text{eV}$ given in Ref. [38].

3. Numerical implementation

The code written in Fortran is parallelized using message parsing interface (MPI). The parallelization is on the geometrical domain of simulation, more specifically on the spatial distribution of main fields (densities, fluxes, electric potential and field) among the processors. Since this is a boundary value problem, all equations can be solved locally if the boundary values are provided. In addition, Poisson's equation is solved iteratively at each time step to compute the electric potential and field.
The system geometry is discretized using a second order centered finite difference scheme. However, classic centered finite difference discretization struggle describing stiff variations of fluxes induced by the boundary conditions and the strong electric fields, thus yields growing and propagating numerical oscillations [39]. In order to overcome numerical instabilities, the vector and scalar quantities are discretized on different grids similar to the finite volume method while keeping the finite difference scheme. In a simulation with N grid points, the scalar quantities are expresses at the normal grid indices $j = 1..N$ while the vectorial quantities have shifted to half indices $j = \frac{3}{2}..N - \frac{1}{2}$. This yields stable solution but the spatial discretization might be improved in the next version of the code by implementing the weighted essentially non oscillatory (WENO) method [40–42] in order to get higher order precision and better numerical stability at the boundaries. The boundaries are treated in a particular way. Only the electric potentials are known at physical boundaries (electrodes) at $j = 0$ and $j = N + 1$. All

other quantities have their boundary conditions defined at $j = \frac{1}{2}$ and $j = N + \frac{1}{2}$ as shown in figure 1:

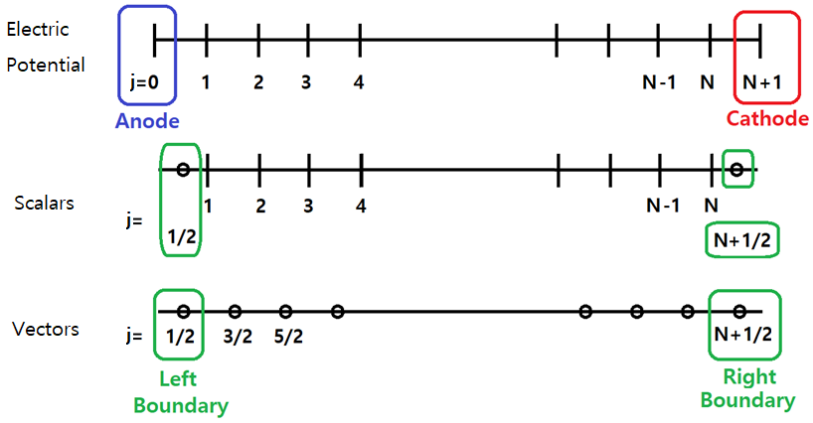

Figure 1: Shifted meshing and boundary definition.

Time resolution is done by explicit strong stability preserving 3rd order Runge-Kutta method (SSP-RK3). The time step Δt is limited by the speed at which physical quantities vary inside the system. As a consequence, the time step Δt has to be smaller than the Maxwell relaxation time [43] in order to correctly describe charged species transport in the system. This relation represents the condition for a slow enough variation of electric field between each time step Δt. Moreover, if there are many physical processes inside the system, the most restrictive space-time resolution should be selected to choose the simulation time order. Finally, Δt and the spatial step Δx are related to each other by the numerical stability constraint of the method used. One common and crucial condition is the Courant-Friedrichs-Lewy (CFL) stability condition [44]:

$$C = u\frac{\Delta t}{\Delta x} \leq C_{max}, \tag{13}$$

where C is called the Courant number and u is the magnitude of the velocity of particles. The value of C_{max} depends on the chosen time integrator. Besides its strong stability preserving property, a four stage SSP-RK3 method also has a C_{max} value twice as big as compared to classic explicit time integrators [45].

4. Simulation results

4.1. Simulation of theoretical plasma sheath

In order to test the code, we first simulated a simplified plasma sheath configuration as described in [46]. We consider the case where the wall has a negative potential with respect to the plasma potential (ion sheath). Assuming a collisionless sheath, Maxwellian electrons and Bohm criterion, the densities of charged particles are expressed

as:

$$n_e(x) = n_s \exp(\frac{e(V(x) - V_s)}{KT_e}), \tag{14}$$

$$n_i(x) = n_s \left[1 - \frac{2e(V(x) - V_s)}{KT_e}\right]^{-\frac{1}{2}}, \tag{15}$$

where $V_s = V_{plasma} - \frac{KT_e}{2e}$ is the electric potential and $n_s = n_{plasma}e^{-0.5}$ is the plasma density at the sheath entrance.

A test simulation was run with the simulation parameters shown in table 1:

Table 1: Test simulation parameters.

L	initial plasma density	initial ε_e	$V_{cathode}$	P	T_{gas}	N_{pts}	dt
3 cm	10^{14} m^{-3}	3 eV	0 V	30 Pa	300 K	300	10^{-12} s

These parameters were chosen in order to simulate a pseudo-post discharge scenario, where we can observe the decay of electron and ion density profiles near the electrodes. Total simulation time was 15 μs, enough time for the electrons to be thermalized with the neutral background gas without reaching the ambipolar diffusion regime which time scale is in order of ms. The comparison of theoretical and numerical density profiles is shown in figure 2:

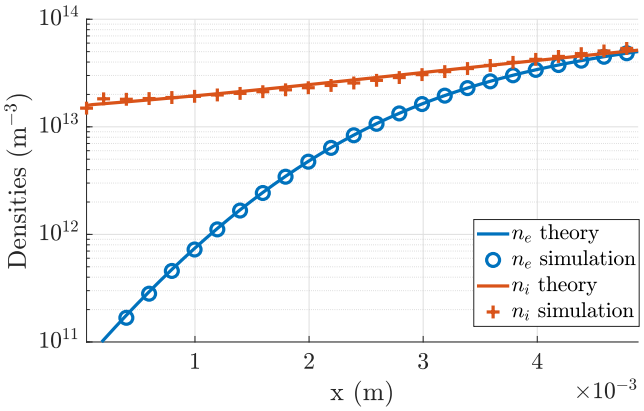

Figure 2: Comparison of sheath density profiles. Red color stands for ions and blue for electrons. Computed electron density is represented by 'o'. Computed ion density is represented by '+'. The plain lines are theoretical sheath density profiles calculated with Eq. 14 and Eq. 15

.

We observe a very good agreement for the electron density profile. The ion density profile shows a good agreement too, except on the first few points near the boundary which show small oscillations. However, this instability does not propagate to the rest of the system during the simulation.

4.2. Simulation of a DC Argon discharge

After recovering the classic sheath density profiles, a DC argon discharge was simulated and compared to PIC results obtained using the commercial VSIM code [24] in order to investigate the physical mechanisms involved in the sheath region and the limits of the fluid model. The simulation parameters are shown in table 2:

Table 2: Simulation parameters.

L	initial plasma density	initial ε_e	$V_{cathode}$	P	T_{gas}	N_{pts}	dt
3 cm	10^{14} m^{-3}	3 eV	-205 V	30 Pa	300 K	1500	10^{-13} s

These parameters are typical to a low temperature DC plasma discharge [47]. The voltage bias has been adjusted according to the breakdown voltage for an argon discharge [48]. The simulation started with a flat density profile in order to test stability. It was run for a few tens of inverse ion plasma frequency, until the system reached a steady state. The main plasma parameters (densities, electric potential, electron mean energy and ion relative velocity profile) are shown in figure 3:

The electric potential profile and electron mean energy profile are close to the expected profile in a low temperature DC plasma discharge [49]. Note the potential fall near the cathode, generating the cathode sheath where electrons are accelerated towards the plasma. Electrons lose their energy due to ionizing collisions in the sheath-plasma interface. However, in the fluid simulation, the peak of ionization is located inside the sheath rather than at its entrance. This might indicate that one is dealing with a collisional sheath in this pressure range. Two slopes in the electron density sheath profile are also observed: the first one from the left is the exponential density decrease and the second one reflects the secondary electron emission from the cathode. While the anode sheath density profiles showed good agreement with the theory, an anomaly is observed in ion density profile in the cathode sheath. This was also backed by the ion relative velocity profile. The ions are too slow compared to the expected order of magnitude of the normalized exit velocity at the cathode: $v_{ion}^{exit,theory} \approx \sqrt{V_{cathode}} \approx 14$.

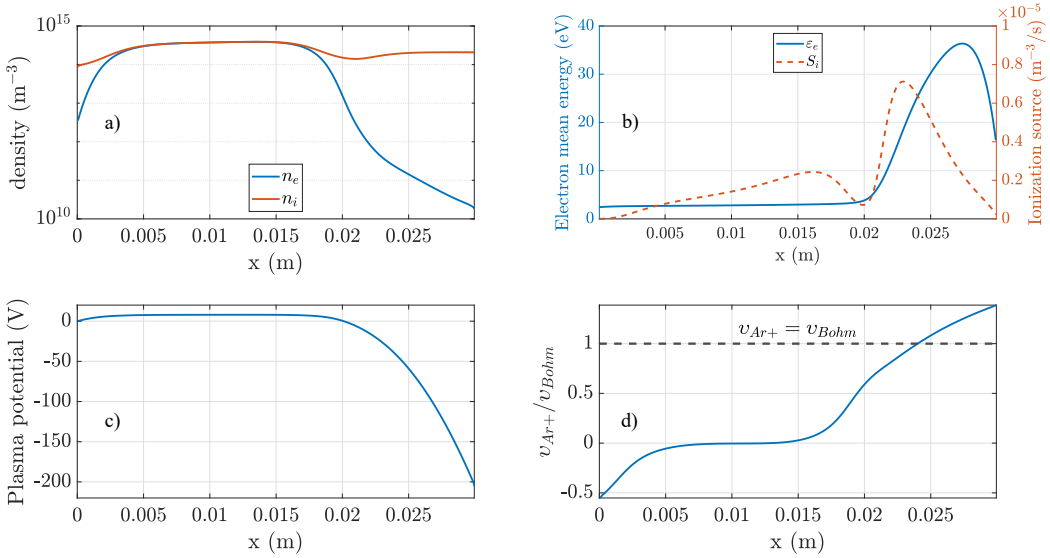

Figure 3: Plasma parameters from 1D DC Argon discharge fluid simulation: a) electron and ion densities, b) electron mean energy and ionization source term, c) plasma potential and d) ion relative velocity.

4.3. Comparison of fluid simulations with PIC simulations for the sheath formation

An anomaly was observed in the sheath region with the fluid model as expected. A particle-in-cell simulation using VSIM/Vorpal [24, 50] was run with similar input parameters in order to investigate the discrepancy between the expected and simulated cathode sheath profile and to identify the main physical mechanism needed for the improvement of the fluid model. The precedent fluid results suggest a collisional sheath at least for the electron-neutral ionizing collisions. A quick estimation of collisionality inside the sheath according to Ref. [51] indicates that there are around 0.8 ion-neutral collisions per Debye length inside the sheath, which is not negligible. Thus, a 1D3v (x,y,z) configuration was chosen in order to investigate the importance of ion-neutral elastic collisions inside the sheath. The results from the 1D3v PIC simulation are presented in figure 4:

We can observe a good agreement with the fluid simulation in electric potential and electron mean energy profiles. The most noticeable difference is the ion density and velocity profiles. The advantage of a PIC simulation is that one has direct access to the ion velocity distribution function. As expected, a shifted velocity distribution in the x direction due to the electric acceleration is observed, and a Maxwellian distribution was observed in the y and z directions. From the width of the distributions functions in the y and z directions, it was found that the ion temperature profile is far from being constant across the simulation domain as shown in the figure 5.a). The assumption of cold ions is clearly falling apart in the sheaths.

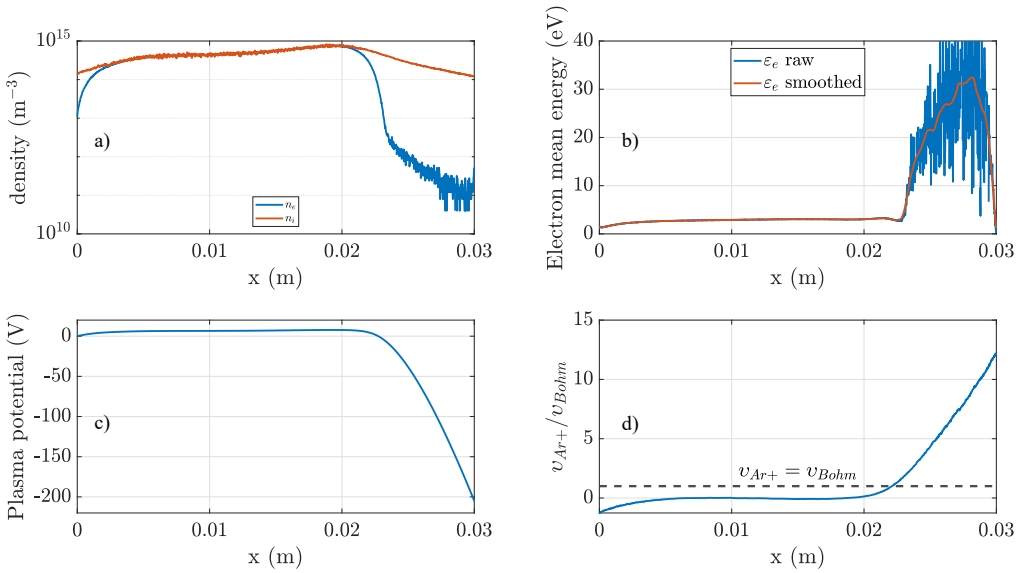

Figure 4: Plasma parameters from 1D DC Argon discharge PIC simulation: a) electron and ion densities, b) electron mean energy, c) plasma potential and d) ion relative velocity.

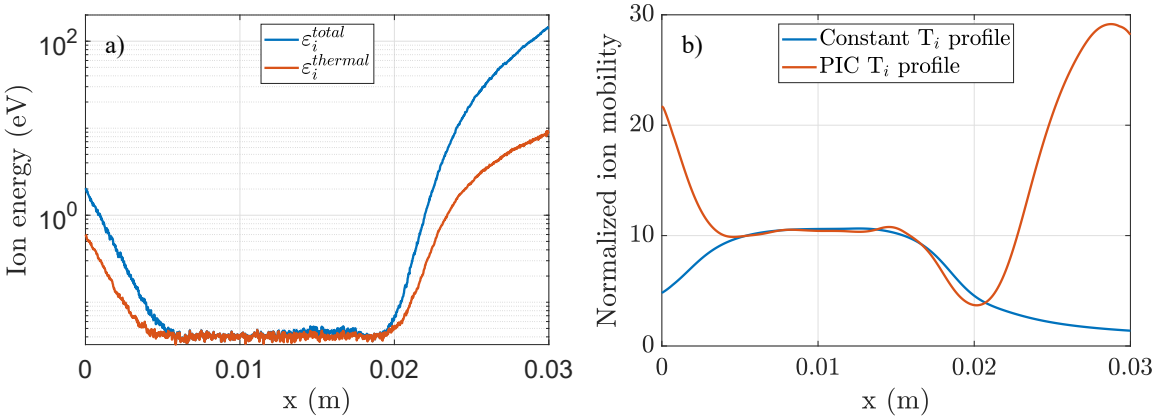

Figure 5: a) Ion total energy and thermal energy profile obtained from PIC simulation, b) Comparison of normalized ion mobility computed in fluid simulation

A new fluid simulation was then ran injecting the ion temperature profile obtained from the PIC simulation inside the fluid code. In order to correctly reflect the influence of a varying ion temperature profile, the modified Frost formula from [36] was adopted. Figure 5.b) shows the comparison of the ion mobility as a function of ion temperature computed by the fluid code. The results of the new fluid simulation are presented in figure 6:

We now observe a better agreement between the two models, including the cathode

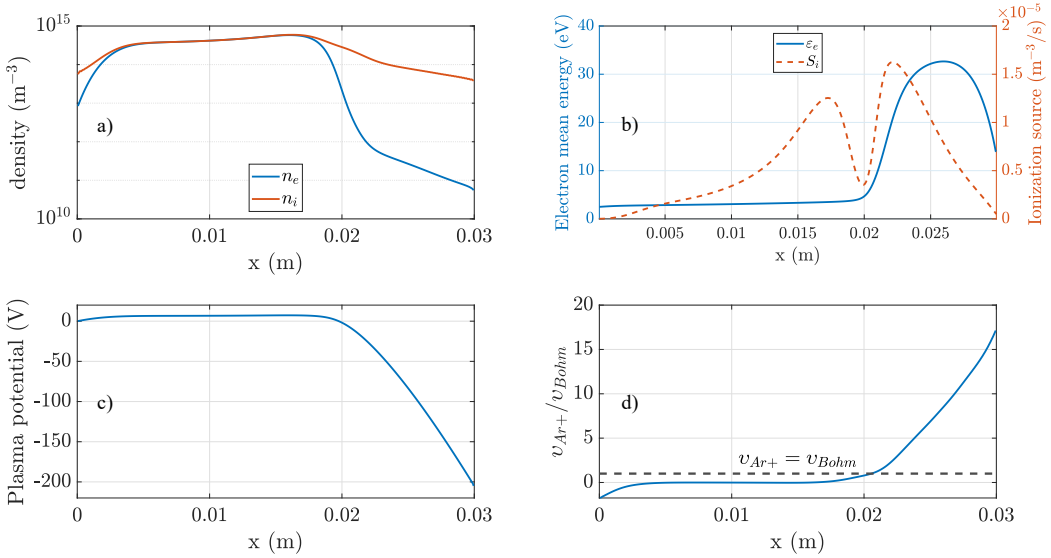

Figure 6: Plasma parameters from 1D DC Argon discharge fluid simulation with injected PIC ion temperature profile: a) electron and ion densities, b) electron mean energy and ionization source term, c) plasma potential and d) ion relative velocity.

sheath profile. It clearly demonstrates the importance of a non constant ion temperature profile and therefore the necessity of the inclusion of the ion energy evolution equation in low temperature plasma fluid model under moderate to high pressure range.

5. Conclusion

This paper presents the preliminary results of a new plasma fluid code currently under development. The code aims at the simulation of the whole discharge including the sheath regions. First one dimensional results of a DC argon discharge show good agreement between theory and simulations (PIC and fluid). In particular, the fluid outputs in the sheath region are greatly improved when a non constant ion temperature profile is considered. It demonstrates the importance of implementing the ion energy evolution equation for low temperature plasma simulation. This result can justify the use of plasma fluid models to study the sheath region. We are currently working on the ion energy evolution equation. The associated collision term will be inspired from the PIC results. A fluid closure concerning the ion heat flux is also necessary. Preliminary results show that one possibility would be to solve the even higher moment equation of heat flux, as done by Hagelaar for the electron heat flux in his fluid model. After improvement of numerical stability and precision and the implementation of the ion energy equation, the code will be used to simulate real experimental devices in order to refine our understanding of the dynamics of the physics of DC plasma discharge. Two dimensional plasma model including magnetic field is currently being developed in order

to study boundary interactions in magnetized sheath region.

Acknowledgements

L.C. and J.H.M. acknowledge the support of the Natural Sciences and Engineering Research Council of Canada (NSERC), Grant No. RGPIN-2019-04333 and would like to thank the Research Computing at the University of Saskatchewan for computational resources on the Plato cluster.

References

[1] Summers C M 1932 *Electrical Engineering* **51** 772–775
[2] Ershov A I, Partlo W N, Bowering N and Hansson B 2009 Laser produced plasma euv light source uS Patent 7,598,509
[3] Goebel D M and Katz I 2008 *Fundamentals of electric propulsion: ion and Hall thrusters* vol 1 (John Wiley & Sons)
[4] Teulet P, Billoux T, Cressault Y, Masquère M, Gleizes A, Revel I, Lepetit B and Peres G 2017 *The European Physical Journal Applied Physics* **77** 20801
[5] Vandamme M, Robert E, Dozias S, Sobilo J, Lerondel S, Pape A and Pouvesle J 2011 *Plasma Medicine* **1** 27–43
[6] Pankaj S K, Bueno-Ferrer C, Misra N, Milosavljević V, O'donnell C, Bourke P, Keener K and Cullen P 2014 *Trends in Food Science & Technology* **35** 5–17
[7] Chen F F 1984 *Introduction to plasma physics and controlled fusion* vol 1 (Springer)
[8] Agency I A E 1988 Establishment of iter: Relevant documents http://inis.iaea.org/search/search.aspx?orig_q=RN:21068957
[9] Langmuir I 1928 *Proceedings of the National Academy of Sciences* **14** 627–637
[10] Hershkowitz N 2005 *Physics of Plasmas* **12** 055502 (*Preprint* https://doi.org/10.1063/1.1887189) URL https://doi.org/10.1063/1.1887189
[11] Riemann K 2008 *Plasma Sources Science and Technology* **18** 014006
[12] Minea T, Bretagne J, Gousset G, Magne L, Pagnon D and Touzeau M 1999 *Surface and Coatings Technology* **116** 558–563
[13] Benstâali W, Belasri A, Hagelaar G and Boeuf J 2008 Calculation of a micro discharge energy balance with pic-mcc method *AIP Conference Proceedings* vol 1047 (AIP) pp 115–118
[14] Debal F, Bretagne J, Dauchot J, Hecq M and Wautelet M 2001 *Plasma Sources Science and Technology* **10** 30
[15] Porokhova I, Golubovskii Y B, Bretagne J, Tichy M and Behnke J 2001 *Physical Review E* **63** 056408
[16] Campanell M D and Umansky M V 2017 *Physics of Plasmas* **24** 057101 (*Preprint* https://doi.org/10.1063/1.4976856) URL https://doi.org/10.1063/1.4976856
[17] Garrigues L, Bareilles J, Boeuf J and Boyd I 2002 *Journal of applied physics* **91** 9521–9528
[18] Hagelaar G, Bareilles J, Garrigues L and Boeuf J P 2003 *Journal of Applied Physics* **93** 67–75
[19] Becker M and Loffhagen D 2013 *AIP Advances* **3** 012108
[20] Becker M M, Kählert H, Sun A, Bonitz M and Loffhagen D 2017 *Plasma Sources Science and Technology* **26** 044001
[21] Baeva M, Loffhagen D, Becker M and Uhrlandt D 2019 *Plasma Chemistry and Plasma Processing* **39** 949–968
[22] Sahu R, Mansour A R and Hara K 2020 *Physics of Plasmas* **27** 113505
[23] Sahu R, Tropina A and Miles R 2022 *Physics of Plasmas* **29** 040701

[24] Tech-X Vsim: Multiphysics simulation software for your complex problems https://www.txcorp.com/vsim/
[25] Delcroix J 1965 Plasma physics
[26] Hagelaar G and Pitchford L C 2005 *Plasma sources science and technology* **14** 722
[27] PITCHFORD L and BOEUF J The siglo database, retrieved on october 17, 2020 http://www.lxcat.net
[28] Hagelaar G Bolsig+ version 122019 http://www.lxcat.net
[29] Richards A D, Thompson B E and Sawin H H 1987 *Applied physics letters* **50** 492–494
[30] Costin C, Marques L, Popa G and Gousset G 2005 *Plasma Sources Science and Technology* **14** 168
[31] Costin C 2005 *Modélisation d'une décharge magnétron DC dans l'argon et en mélanges argon-oxygène par un modèle fluide* Ph.D. thesis Paris 11
[32] Salabas A, Gousset G and Alves L 2002 *Plasma Sources Science and Technology* **11** 448
[33] Ellis H, Pai R, McDaniel E, Mason E and Viehland L 1976 *Atomic data and nuclear data tables* **17** 177–210
[34] Phelps A V 1991 *Journal of Physical and Chemical Reference Data* **20** 557–573
[35] Frost L 1957 *Physical Review* **105** 354
[36] Khrapak A G, Golyatina R, Maiorov S and Khrapak S A 2020 *High Temperature* **58** 545–549
[37] Phelps A and Petrovic Z L 1999 *Plasma Sources Science and Technology* **8** R21
[38] Chapman B 1980 Glow discharge processes
[39] Hagelaar G and Kroesen G 2000 *Journal of Computational Physics* **159** 1–12
[40] Liu X D, Osher S and Chan T 1994 *Journal of computational physics* **115** 200–212
[41] Jiang G S and Shu C W 1996 *Journal of computational physics* **126** 202–228
[42] Shu C W 2009 *SIAM review* **51** 82–126
[43] Barnes M S, Cotler T J and Elta M E 1987 *Journal of applied physics* **61** 81–89
[44] Courant R, Friedrichs K and Lewy H 1967 *IBM journal of Research and Development* **11** 215–234
[45] Durran D R 2010 *Numerical methods for fluid dynamics: With applications to geophysics* vol 32 (Springer Science & Business Media)
[46] Moisan M and Pelletier J 2012 *Physics of Collisional Plasmas: Introduction to high-frequency discharges*
[47] Couëdel L, Arnas C *et al.* 2014 *Journal of Plasma Physics* **80** 849
[48] Ibrahim W 2017 **20**
[49] Raizer Y P and Allen J E 1991 *Gas discharge physics* vol 1 (Springer)
[50] Nieter C and Cary J R 2004 *Journal of Computational Physics* **196** 448–473
[51] Sheridan T E and Goree J 1991 *Physics of Fluids B: Plasma Physics* **3** 2796–2804 (*Preprint* https://doi.org/10.1063/1.859987) URL https://doi.org/10.1063/1.859987